iScience

CellPress
OPEN ACCESS

Article

Lotus-root-shaped cell-encapsulated construct as a retrieval graft for long-term transplantation of human iPSC-derived β-cells

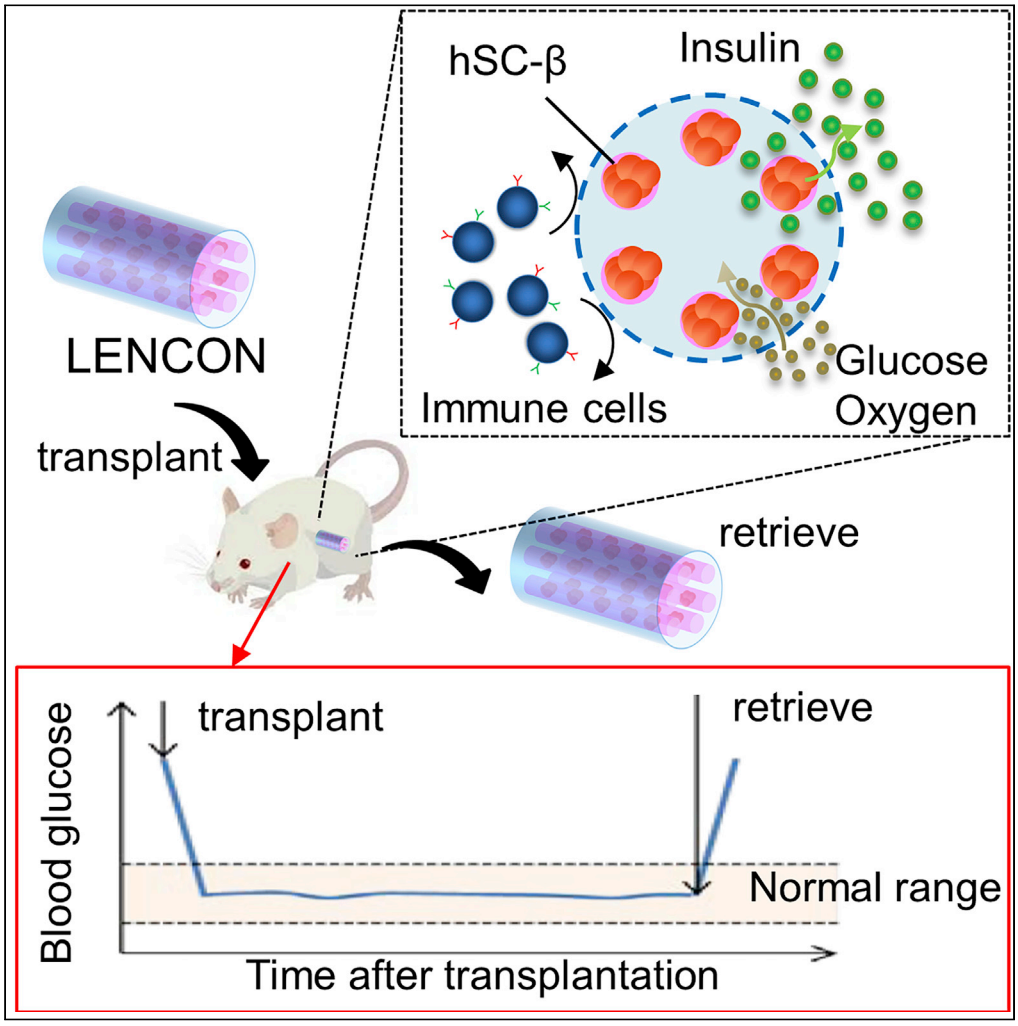

Fumisato Ozawa, Shogo Nagata, Haruka Oda, Shigeharu G. Yabe, Hitoshi Okochi, Shoji Takeuchi

takeuchi@hybrid.t.u-tokyo.ac.jp

Highlights

A lotus-root-shaped cell-encapsulated construct as a retrieval graft

Advantages in terms of FBR mitigation and mechanical strength as a graft

Control the recipient blood glucose levels of NOD-Scid mice for up to half a year

Retrieval without adhesion over 1 year after transplantation

Ozawa et al., iScience 24, 102309
April 23, 2021
https://doi.org/10.1016/j.isci.2021.102309

iScience

CellPress
OPEN ACCESS

Article

Lotus-root-shaped cell-encapsulated construct as a retrieval graft for long-term transplantation of human iPSC-derived β-cells

Fumisato Ozawa,[1] Shogo Nagata,[1] Haruka Oda,[2] Shigeharu G. Yabe,[3] Hitoshi Okochi,[3] and Shoji Takeuchi[1,2,4,*]

SUMMARY

Cell therapy using human-stem-cell-derived pancreatic beta cells (hSC-βs) is a potential treatment method for type 1 diabetes mellitus (T1D). For therapeutic safety, hSC-βs need encapsulation in grafts that are scalable and retrievable. In this study, we developed a lotus-root-shaped cell-encapsulated construct (LENCON) as a graft that can be retrieved after long-term hSC-β transplantation. This graft had six multicores encapsulating hSC-βs located within 1 mm from the edge. It controlled the recipient blood glucose levels for a long-term, following transplantation in immunodeficient diabetic mice. LENCON xenotransplanted into immunocompetent mice exhibited retrievability and maintained the functionality of hSC-βs for over 1 year after transplantation. We believe that LENCON can contribute to the treatment of T1D through long-term transplantation of hSC-βs and in many other forms of cell therapy.

INTRODUCTION

Diabetes mellitus affects over 400 million patients globally. It causes complications, such as kidney damage, visual impairment, and neuropathy. There are several treatments available for type 1 diabetes mellitus (T1D), such as daily injections of exogenous insulin (Hirsch 1999, Swinnen et al., 2009), pancreatic transplantation (Gruessner and Sutherland, 2005, Hampson et al., 2010), and cell therapy (McBane et al., 2013, Amer and Bryant, 2016, Ellis et al., 2013, Elliott et al., 2007, Bochenek et al., 2018). Cell therapy using human-stem-cell-derived pancreatic beta cells (hSC-βs) is attracting attention for donor-independent islet transplantation (Hogrebe et al., 2020, Rezania et al., 2014, Pagliuca et al., 2014, Yabe et al., 2019). In previous studies, transplantation was performed using encapsulated hSC-β grafts in mice and non-human primates (Agulnick et al., 2015, Vegas et al., 2016, Fukuda et al., 2019, Berman et al., 2016). A graft for clinical application should be scalable, for encapsulating many cells in a single piece and retrievable after transplantation, for therapeutic safety. Retrievable grafts should allow removal without adhesion and should be sufficiently strong to maintain their shape for a long time *in vivo*. Retrievable grafts of mouse and rat primary cells have been proposed (Onoe et al., 2013, Ma et al., 2013, Tomei et al., 2014, Watanabe et al., 2020); however, there is no report on hSC-β grafts that retain their function for a long time after transplantation. The previous grafts encapsulating hSC-βs induced intense foreign-body responses (FBRs), compared to those encapsulating human primary islets (Torren et al., 2017), resulting in fibrotic deposition, adhesion, nutrient isolation, and cell death.

In this study, we develop a lotus-root-shaped cell-encapsulated construct (LENCON) as a graft that can be retrieved after long-term (>1 year) hSC-β transplantation. Figure 1 shows the structure of the proposed LENCON with millimeter-thickness. Grafts with millimeter-thickness tend to mitigate FBR (Watanabe et al., 2020, Veiseh et al., 2015), as well as exhibit higher mechanical strength. The cells are placed near the edge of the lotus-root-shaped graft structure to support cell survival. When the diameter of the graft is in the order of millimeters or more, the diffusion of oxygen and nutrients from the surrounding hydrogel throughout the encapsulated cells is limited resulting in cell death in the center of the hydrogel (Li et al., 1995, Weaver et al., 2018, Buchwald et al., 2018). In addition, this graft is scalable in the direction of the long axis; and therefore, the number of cells can be increased. Here, we fabricate LENCON and evaluate the survival of the encapsulated cells. We then transplant the grafts into mice and characterize cell function, graft strength, and retrievability.

[1]Institute of Industrial Science, The University of Tokyo, 4-6-1 Komaba, Meguro-ku, Tokyo 153-8505, Japan

[2]Graduate School of Information Science and Technology, The University of Tokyo, 7-3-1 Hongo, Bunkyo-ku, Tokyo 113-8656, Japan

[3]Department of Regenerative Medicine, Research Institute, National Center for Global Health and Medicine, 1-21-1 Toyama, Shinjuku-ku, Tokyo 162-8655, Japan

[4]Lead contact

*Correspondence: takeuchi@hybrid.t.u-tokyo.ac.jp

https://doi.org/10.1016/j.isci.2021.102309

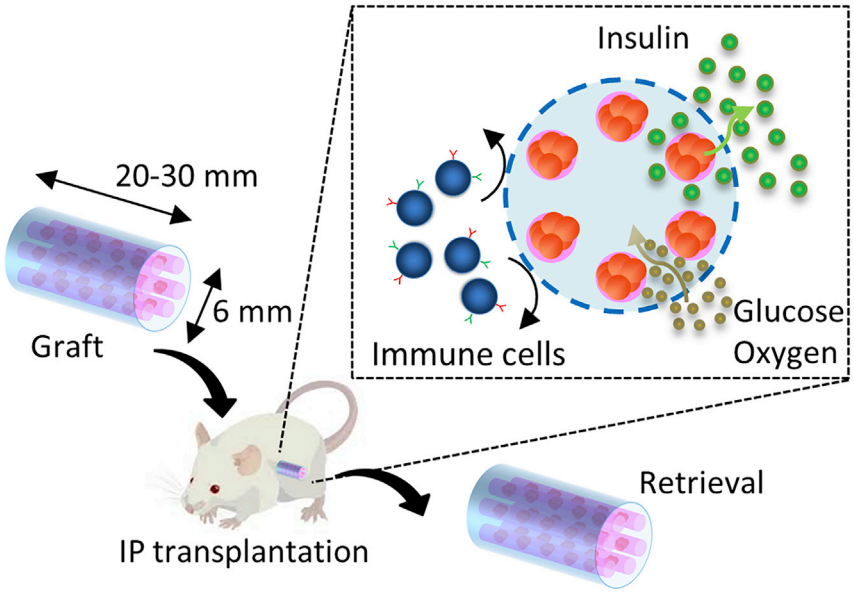

Figure 1. Concept of LENCON transplantation

RESULTS

Optimization of LENCON

For millimeter-thick fiber-encapsulation of cells, we employed a lotus-root like geometry, in which cells are placed near the edges of the grafts, enabling cell survival, and are covered by a Ba-alginate hydrogel shell. To determine the cell position from the edge, we fabricated 6-mm-thick fibers encapsulating hSC-βs with randomized cell positions in the hydrogel. After a 1-week culture, we prepared hematoxylin and eosin (HE)-stained sections of the 6-mm-thick fibers and estimated the survival ratio by dividing the number of enucleated cells by the total number of cells in the HE sections. The live cell area was calculated as the cell area obtained by subtracting the area occupied by enucleated cells from the area occupied by all stained cells; we postulated that cells without enucleation are viable cells. The cells within 1 mm from the edge of the fabricated LENCON maintained 80% ± 12% nuclear staining, while the cells over 1 mm from the edge exhibited significantly increased enucleation (Figure 2A), suggesting that most cells within 1 mm from the edge were viable cells.

Using a fluidic device, LENCON was fabricated, as shown in the transparent methods section (Figure S1) and Video S1. The LENCON had a diameter of 6 mm and six multicores encapsulating hSC-βs (Figures 2B–2E). Each core had a diameter of 600–700 μm and was located within 1 mm from the edge (Figure 2F). The live/dead fluorescent staining (Figure 2G) indicated that most of the stained hSC-βs in LENCON were viable before transplantation. Moreover, immunofluorescence images revealed that human C-peptide-positive cells were present even after encapsulation (Figure S2). These results suggested that the encapsulation process was sufficient to maintain hSC-β survival and function.

Effect of graft size on FBR and mechanical stability in immunocompetent mice

To investigate the effects of the size of graft encapsulating hSC-βs, we compared the FBR based on the degree of cell deposition in the graft, and the adhesion between the host tissue and graft. We prepared 1-mm-thick grafts and 6-mm-thick LENCONs. Each graft was transplanted into immunocompetent C57BL/6 mice and retrieved after 2 months, 4 months, and 1 year. Four months after transplantation, the 1-mm-thick graft exhibited intense cell deposition and adhesion to the recipient mouse tissue (Figures 3A, 3B, and 3E); it was retrieved with peeling off at the adhesion site (Figure 3B). In contrast, the 6-mm-thick LENCON did not exhibit intense cell deposition (Figure 3C) and could be retrieved without obvious adhesion (Figure 3D). We compared the thickness of the cell deposition using images of HE-stained sections (Figures 3E–3H). The 1-mm-thick grafts were surrounded by an approximately 400-μm-thick cell deposition (Figures 3E and 3I), while the 6-mm-thick LENCON was only partially covered by cells, with a deposition as

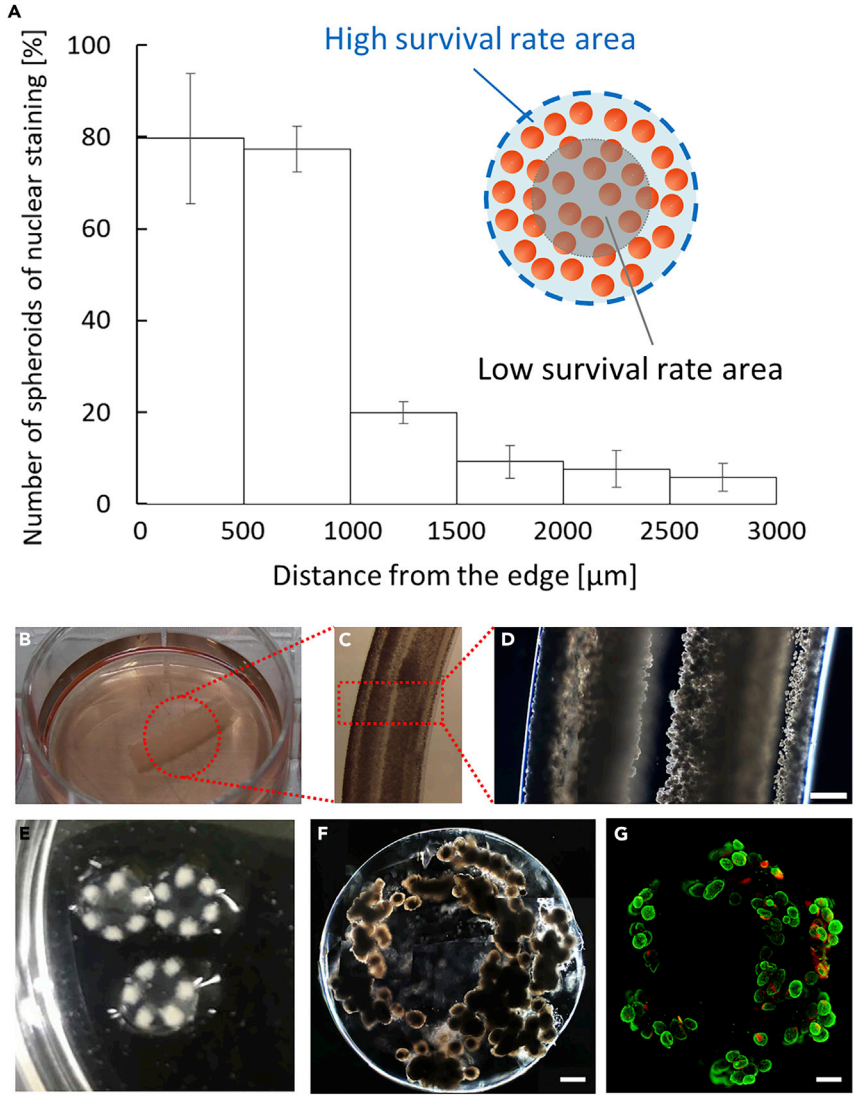

Figure 2. Formation of LENCON

(A) Survival of hSC-βs in a 6-mm-thick hydrogel after one week of culture.

(B) Optical images of the long axis direction of the 6-mm-thick LENCON.

(C and D) Microscopic images of the long axis direction of the 6 mm-thick LENCON.

(E) Optical images of the short axis direction of the 6-mm-thick LENCON.

(F) Microscopic images of the 6-mm-thick LENCON. (Scale bar: 500 μm).

(G) Fluorescent staining images of 6-mm-thick LENCON stained with calcein-AM and propidium iodide. (Scale bar: 500 μm)

thin as 20 μm (Figures 3F and 3I). The degree of cell deposition also affects the survival of encapsulated cells; the hSC-βs in the 1-mm-thick grafts were enucleated and dead (Figure 3F), while those in the 6-mm-thick LENCONs retained their nuclei and were viable (Figure 3H). These results indicate that the 6-mm-thick LENCONs provide an appropriate microenvironment to hSC-βs during transplantation.

To evaluate the changes in mechanical stability of the graft before and after transplantation, we measured the elastic modulus of each graft using a rheometer (Figure 3J). Both the 1-mm- and 6-mm-thick grafts showed similar elastic modulus before transplantation. However, after transplantation, the 1-mm-thick graft exhibited a significantly reduced elastic modulus, and its storage modulus became lower than the loss modulus, indicating that the state of the graft changed from gel to sol after 4 months of transplantation. After 1 year of transplantation, the 1-mm-thick grafts were too fragile to be retrieved, and we were

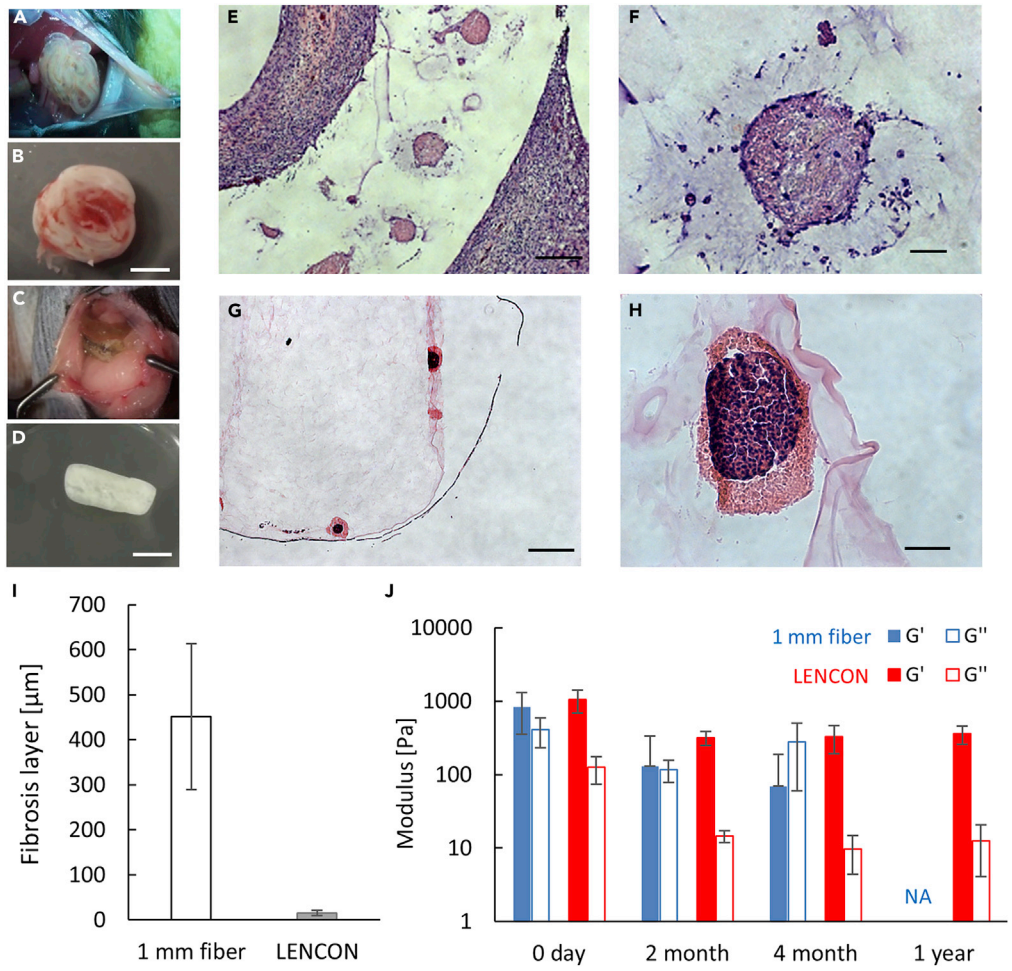

Figure 3. Evaluation of fibrosis formation and mechanical strength of grafts

(A) Second-look laparotomy of the mice transplanted with 1-mm-thick grafts. The 1 mm-thick grafts adhered to the recipient mice.

(B) Retrieved 1-mm-thick grafts. The grafts were covered with thick cell layers.

(C) Second-look laparotomy of the recipient mice transplanted with 6-mm-thick LENCONs. The 6-mm-thick grafts did not obviously adhere to the recipient mice.

(D) Retrieved 6-mm-thick LENCONs. The grafts were partially deposited with thin cell layers.

(E) HE-stained sectional image of retrieved 1-mm-thick grafts.

(F) Enlarged HE-stained sectional image of retrieved 1-mm-thick grafts.

(G) HE-stained sectional image of retrieved 6-mm-thick LENCONs.

(H) Enlarged HE-stained sectional image of retrieved 6 mm-thick LENCONs. Scale bars: (E, G) 1 mm, (F, H) 50 μm. Time points of images a-h, 4 months after transplantation.

(I) Comparison of fibrosis layer deposition.

(J) Rheological measurements of the each retrieved graft. (NA: The 1-mm-thick grafts 1 year after transplantation were too fragile to be retrieved.)

unable to perform a rheological analysis. In contrast, the elastic modulus of the 6-mm-thick grafts decreased slightly in the beginning but showed negligible decrease after 2 months, and the storage modulus was higher than the loss modulus, indicating that the grafts maintained the gel-state after 2 months, 4 months, and 1 year of transplantation.

Long-term transplantation of LENCON in immunodeficient mice

To confirm the *in vivo* functionality of LENCON encapsulating hSC-βs (6×10^6 cells) with reduced transplant rejection, we transplanted the LENCONs into the intraperitoneal space of normal immunodeficient NOD-

Scid mice (Figures 4A–4C and Video S2). After transplantation, the human C-peptide concentration in blood gradually increased (Figure 4D), as in the case of the 1 mm-thick graft (Figure S3), suggesting that the hSC-βs in the LENCON were functional during transplantation. We performed second-look laparotomy and retrieved the grafts after over 28 weeks of transplantation (Video S3). All grafts appeared intact in the recipient's abdominal cavities without adhesion to the recipient's adjacent abdominal tissues (Figure 4E). In addition, the grafts could be retrieved from the intraperitoneal space of the recipients (Figure 4F). The retrieved grafts had viable hSC-βs (Figures 4G and S4), while the 1-mm-thick grafts encapsulating hSC-βs were broken into pieces in the intraperitoneal space and could not be retrieved completely (Figure S5).

To demonstrate the glycemic control potential, we measured the blood glucose levels of the recipient streptozotocin (STZ)-induced diabetic mice daily after transplantation of the LENCON. We hypothesized that the glycemic control in the recipient mice is highly correlated with the functions of hSC-βs. We transplanted LENCON encapsulating hSC-βs into the intraperitoneal space of STZ-induced diabetic mice and monitored their non-fasting blood glucose concentrations (Figure 4H). The recipients with LENCON transplantation exhibited normoglycemia within 10 days post-transplantation. Subsequently, the recipient mice with transplanted LENCONs maintained normoglycemia, while all recipient mice without the grafts were hyperglycemic. In addition, the glucose tolerance levels of LENCON-transplanted mice were comparable to those of normal mice even after 100 days of transplantation (Figures 4I and 4J). We performed second-look laparotomy and retrieved the grafts after 56 days, 120 days, 130 days, 136 days, and 180 days of transplantation. All grafts appeared intact in the recipient's abdominal cavities without adhesion to the recipient's adjacent abdominal tissues similar to non-diabetic mice. In addition, the grafts could be retrieved from the intraperitoneal space of the recipients, which resulted in the reappearance of hyperglycemia in the recipients. The retrieved grafts were evaluated using a glucose-stimulated insulin secretion assay, and their functionalities before and after transplantation were compared (Figure S6). LENCONs encapsulating hSC-βs maintained their function of controlling the blood glucose concentration even after transplantation and retrieval.

Long-term xenotransplantation of LENCON in immunocompetent mice

To evaluate whether the LENCONs can be transplanted for a long duration, while maintaining intact immune systems, we transplanted LENCONs encapsulating hSC-βs into the intraperitoneal space of immunocompetent C57BL/6 mice (Figures 5A–5C). After 1 year of transplantation, we performed second-look laparotomy and retrieved the grafts (Figures 5E and 5G). Nine out of the ten LENCONs transplanted were successfully retrieved without adhesion to the recipient's adjacent abdominal tissues (Video S4). The retrieved LENCONs remained intact, although some parts of the graft exhibited a thin cell layer and the edge was slightly rounded (Figure 5G). No tumor formation was observed in the recipient mice due to cell leakage. These results suggest that LENCONs exhibit retrievability and therapeutic safety even in immunocompetent mice.

During the transplantation period, we collected blood of the recipient mice every two weeks and measured the levels of human C-peptide using ELISA. The human C-peptide levels in blood were intermittently detected over the 50-week transplantation period (Figure 5D). The retrieved LENCON sustained the human C-peptide-positive hSC-βs as indicated through HE and immunostaining (Figures 5H and 5I). In addition, the encapsulated cells expressed other islet markers (Figure S7). Following the glucose-stimulated insulin secretion (GSIS) assay (Figure 5J); both human C-peptide and glucagon were secreted in response to the glucose stimulation, indicating that functional hSC-βs survived in the LENCONs for more than 1 year. These results corroborate that our LENCON has a high potential for long-term xenotransplantation of functional hSC-βs.

DISCUSSION

In this study, we developed 6 mm-thick LENCONs for long-term transplantation, which had six multicores encapsulating hSC-βs located within 1 mm from the edge. The LENCON transplanted into immunodeficient mice controlled the recipient blood-glucose concentration for a period of 180 days after transplantation. The LENCON xenotransplanted into immunocompetent mice maintained retrievability and hSC-β functionality for over a year after transplantation.

Recently, it was reported that hydrogel capsules larger than 1-mm-thick tend to mitigate FBR (Watanabe et al., 2020, Veiseh et al., 2015). In our experiment, however, when 1-mm-thick grafts encapsulating hSC-βs

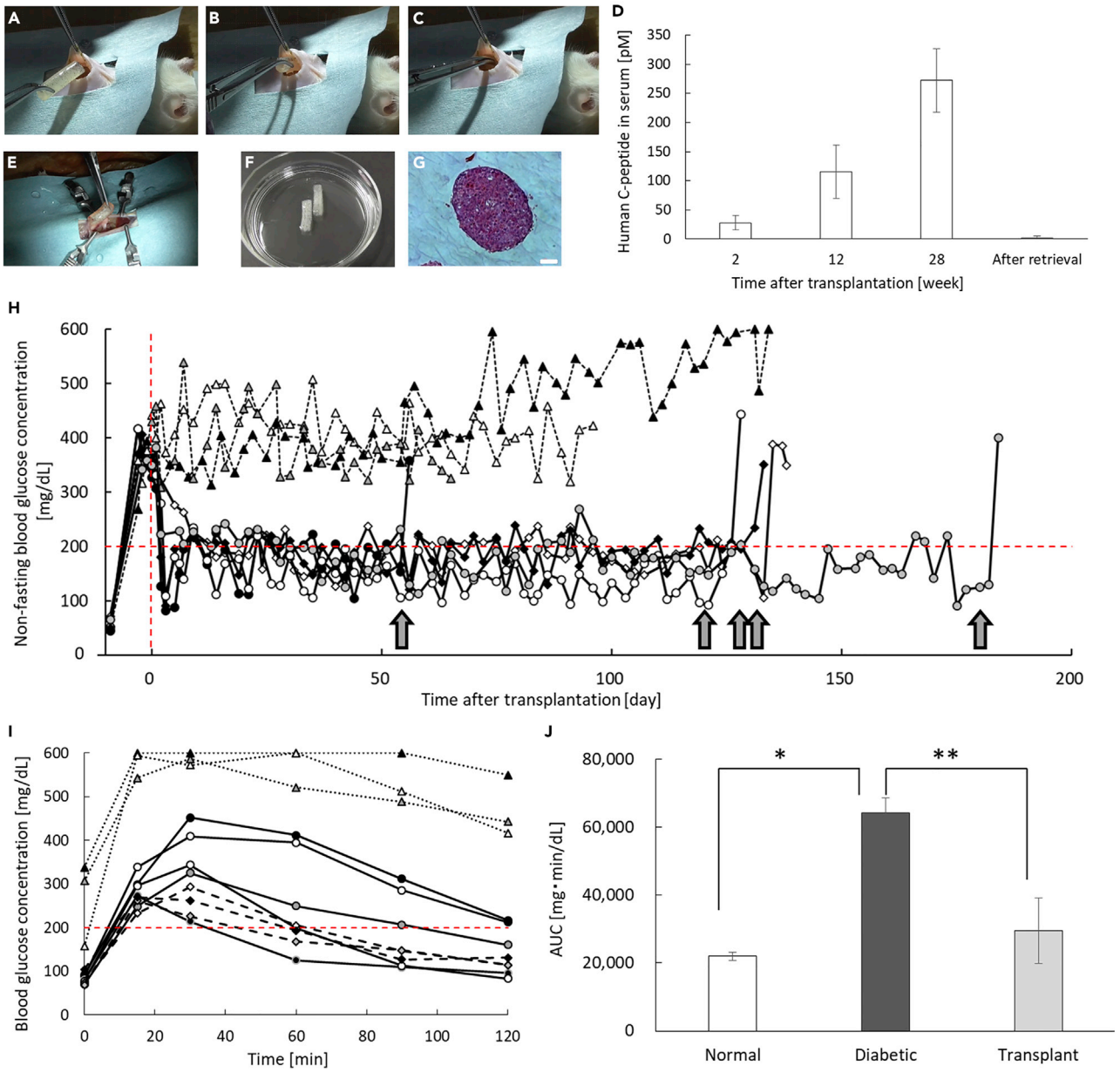

Figure 4. *In vivo* demonstration of therapeutic potential of the LENCON using NOD-Scid mice

(A–C) Laparotomy of transplantation of the LENCON.

(D) ELISA results of blood samples of the recipient mice.

(E) Second-look laparotomy for retrieval of the LENCON.

(F) Optical image of retrieved LENCON.

(G) HE-stained sectional image of hSC-βs in the retrieved LENCONs. (Scale bar: 50 μm).

(H) Changes in the non-fasting blood glucose concentration of mice transplanted with the LENCONs (solid line: LENCON transplantation, N = 5, dotted line: non-transplantation, N = 3). The transplanted grafts in the intraperitoneal cavities were retrieved at the timepoints indicated by the arrows (days 54, 120, 127, 131, and 180).

(I) Oral glucose tolerance test (OGTT) results of recipient mice 7 days before retrieval (solid line: recipient mice with LENCON transplantation, N = 5, dotted line: diabetic mice without transplantation, N = 3, dashed line: normal mice, N = 3).

(J) The area under curve of the plasma glucose concentrations during OGTT of recipient mice (N = 3).

were transplanted into mice, the grafts showed intense FBR. This result is possibly due to the considerable difference between mice and humans; hSC-βs induce severe inflammation than the previously used cells (e.g., mouse/rat primary islets). We found that the 6-mm-thick LENCON tended to mitigate FBR even

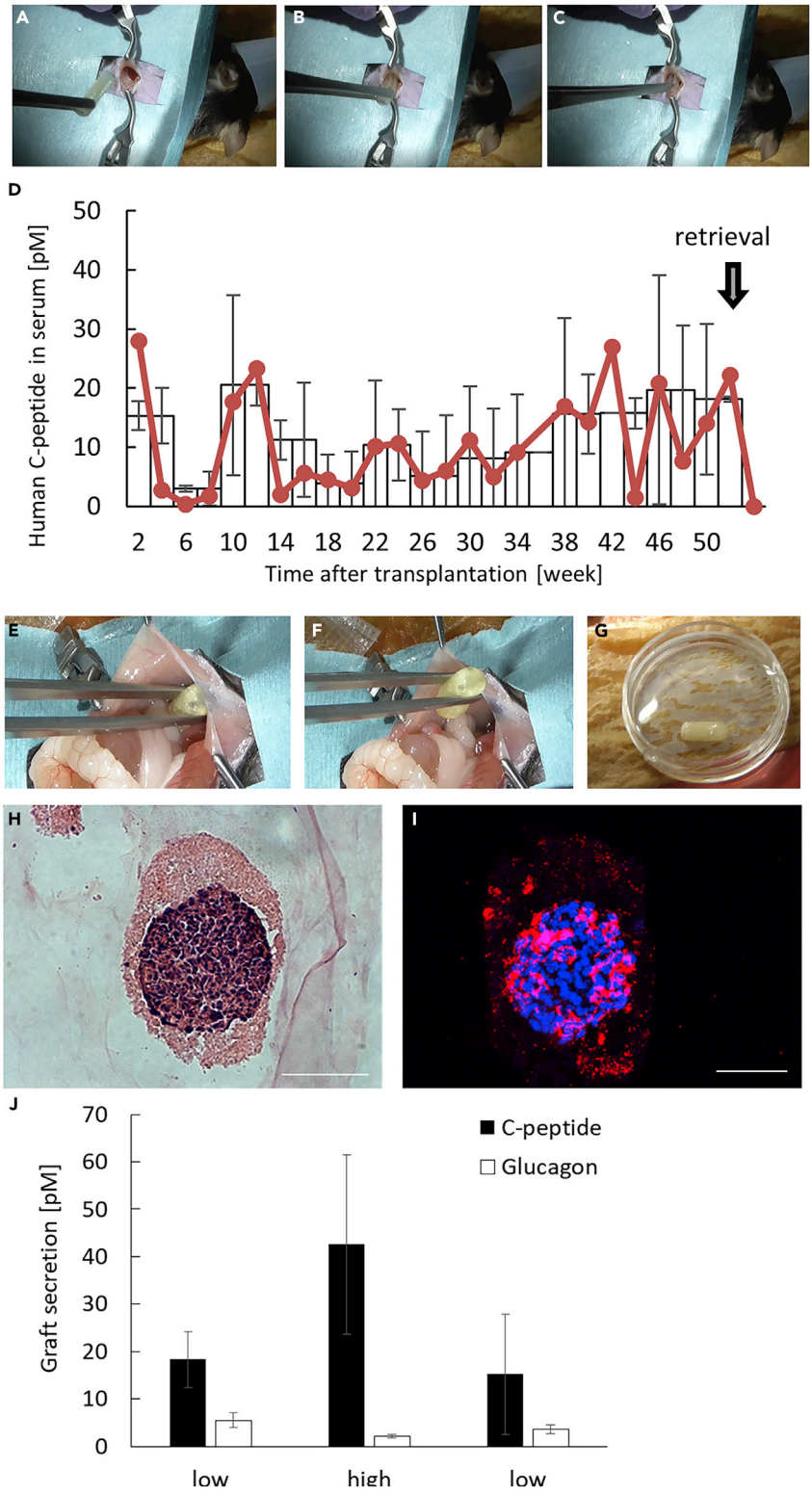

Figure 5. Long-term transplantation of LENCON into immunocompetent C57BL/6 mice

(A–C) Laparotomy of transplantation of the LENCON.

(D) ELISA results of blood samples of recipient mice.

Figure 5. *Continued*
(E and F) Second-look laparotomy for retrieval of the LENCON.
(G) Optical image of retrieved LENCON.
(H) HE-stained sectional images of hSC-β in the retrieved LENCON. (Scale bar: 50 μm).
(I) Fluorescent images of hSC-β in the retrieved LENCON stained for C-peptide. (Scale bar: 50 μm).
(J) Glucose responsive test of the retrieved LENCONs.

when encapsulating hSC-βs. We did not elucidate the mechanism through which larger grafts mitigate FBR; however, the relationship between graft size and macrophage functions may help us understand this interesting phenomenon. Millimeter order grafts are surrounded by only a few macrophages, resulting in reduced recruitment and extravasation of additional macrophages (Vegas et al., 2016, Veiseh et al., 2015). In the case of hSC-βs, a thickness of 1 mm was presumably not sufficient to prevent macrophage recruitment, but a thickness of 6 mm was. This fact could lead to a design concept, larger thickness is better to mitigate FBR, while it may increase the burden on the host recipients. Therefore, our results strongly suggest that there may be an optimal graft size depending on the encapsulated cells and host animals.

The 6 mm-thick LENCONs have advantages in terms of mechanical strength over the thinner LENCONs. In case of thin fibers, the fibers bend easily and they are eventually entangled after the transplantation; this increase in the shape complexity may promote cell deposition on the surface of the graft. In contrast, the 6-mm-thick LENCONs do not bend *in vivo* because of the increased mechanical strength, thereby mitigating cell deposition. In addition, it is known that the cell deposition can be mitigated by modifying the alginate (Liu et al., 2019, Yang et al., 2019) and other chemicals (Doloff et al., 2017, Farah et al., 2019, Alagpulinsa et al., 2019, Kikawa et al., 2014). Combining these materials with mechanically strong LENCONs will provide more inert grafts.

In addition to influencing FBR, increase in the graft size influences cell survival; cells may die, as nutrients and oxygen do not reach the encapsulated cells located at the center of the grafts, resulting in the dysfunction of the graft. We showed that the hSC-βs encapsulated within 1 mm from the edge of the graft could receive sufficient supply oxygen and nutrients during transplantation. The lotus-root-like geometry of our LENCON enables adequate supply of oxygen and nutrients to the encapsulated cells near the edge of the graft, despite the larger size of the graft. The levels of C-peptide at 12 weeks post-transplantation did not exhibit a significant difference between the control 1 mm graft and the LENCON. This indicates that insulin secretion from the LENCON was sufficient as comparable to the previously reported encapsulation devices (Fukuda et al., 2019). In addition, by modifying the graft to be hollow in the center, it will be possible to supply oxygen and nutrients from the edges to the center and enhance the graft functions.

More cells than those required for transplantation into mice need to be encapsulated for clinical transplantation in humans (Park et al., 2015, Sphapiro et al., 2006). Scaling up the number of cells would be problematic when using hydrogel beads, in terms of retrievability. Ensuring complete retrieval of the hydrogel beads is challenging because of the large capsule numbers and the complicated organ structures of the abdominal cavity. However, our LENCON could be scaled up as one graft by increasing the number of cores and the length of the graft, and thereby improving the retrievability of the grafts.

For cell therapy using stem cell-derived cells, the long-term graft functions and the therapeutic safety need to be considered. First, in long-term transplantation, the LENCON encapsulating hSC-βs can control the blood glucose concentrations of recipient mice with deficient immune systems. The increase in blood C-peptide production during transplantation suggests that the encapsulated hSC-βs became more mature *in vivo*; this result is consistent with that reported by recent studies on hSC-β transplantations (Rezania et al., 2014, Pagliuca et al., 2014, Yabe et al., 2019, Fukuda et al., 2019). Challenges remain in controlling the blood glucose concentration, considering the large species difference; however, the LENCONs represent a major advancement in cell therapy in terms of the survival of encapsulated hSC-βs and their retrievability over 1 year after transplantation in immunocompetent mice. Macrophages and activated fibroblasts, which promote inflammation and fibrosis, were attached to a part of the graft surface after long-term transplantation, as observed through immunofluorescent staining (Figure S8). These cells might cause FBR and induce a decline in graft function (Veiseh et al., 2015, Watanabe et al., 2020). We believe that optimizing the structure of the graft and replacing the hydrogel with a more hydrophilic material may mitigate such cell deposition. Second, our study shows that the LENCONs are therapeutically safe because no apparent tumor formation was observed in the host recipient mice, and these grafts can be used in other

stem-cell-derived endocrine cell transplantations, such as hypophysis and thyroid transplantation. The LENCON encapsulating hSC-βs can be a powerful tool with minimal risks for the treatment of T1D and can be potentially used in several other forms of cell therapy that require graft retrievability.

Limitations of the study

Some limitations of this study must be acknowledged. In human clinical application, the encapsulated cells in the graft should be more, around 500,000 IEQ of human primary islets. The functionality of hSC-βs is inferior to that of human primary islets, and a larger number of hSC-βs are required. It is expected that the required number of cells in a LENCON will be similar to that required for human primary islets, considering the improved function of hSC-βs. The LENCON should be optimized for human applications by increasing the number of cores, their diameter, and the length of the graft. Host FBR to the graft are another limitation. The alginate hydrogel does not completely mitigate FBR and cannot completely control the blood glucose levels of immunocompetent mice. A zwitterionically modified alginate hydrogel and other chemicals that reduce inflammatory effects could alleviate this problem. The alginate hydrogel could be replaced with a hydrophilic hydrogel exhibiting low protein adsorption affinity.

Resource availability

Lead contact

Further information and requests for resources and reagents should be directed to and will be fulfilled by the lead contact, Shoji Takeuchi (takeuchi@hybrid.t.u-tokyo.ac.jp).

Materials availability

Not applicable.

Data and code availability

Not applicable.

METHODS

All methods can be found in the accompanying transparent methods supplemental file.

SUPPLEMENTAL INFORMATION

Supplemental information can be found online at https://doi.org/10.1016/j.isci.2021.102309.

ACKNOWLEDGMENTS

We thank H. Aoyagi and A. Takimoto for their assistance with the maintenance of diabetic mice, measurement of daily blood glucose concentrations, and preparation of the frozen sections of grafts. We also thank T. Saito for assistance with the fabrication of fluidic devices and LENCONs. This work was partly supported by Research Center Network for Realization of Regenerative Medicine (19bm0304005h0007), Japan Agency for Medical Research and Development (AMED), Japan, and Grant-in-Aid for Scientific Research (S) (Grant number: 16H06329) and Grant-in-Aid for Early-Career Scientists (Grant number: 19K20664) Japan Science and Technology (JST), Japan.

AUTHOR CONTRIBUTIONS

F. Ozawa and S. Takeuchi conceived the design of the study. F. Ozawa fabricated the fluidic devices and grafts. F. Ozawa and S. Nagata designed and conducted graft transplantation experiments in mice. H. Oda measured the elastic modulus of grafts. S. Yabe and H. Okochi prepared the hSC-βs. F. Ozawa analyzed the grafts via microscopy observations of HE sections. S. Nagata analyzed the grafts through confocal microscopy and recorded the immunofluorescent images. All authors discussed the results and commented on the manuscript.

DECLARATION OF INTERESTS

S. Takeuchi is an inventor on intellectual property rights related to the cell fiber technology, and stockholders of Cellfiber Inc, a start-up company based on the cell fiber technology. However, any authors

are NOT employed by the commercial company: Cellfiber Inc. Thus, this does not alter our adherence to iScience policies on sharing data and materials.

Received: August 24, 2020
Revised: November 16, 2020
Accepted: March 11, 2021
Published: April 1, 2021

REFERENCES

Agulnick, A.D., Ambruzs, D.M., Moorman, M.A., Bhoumik, A., Cesario, R.M., Payne, J.K., Kelly, J.R., Haakmeester, C., Srijemac, R., Wilson, A.Z., et al. (2015). Insulin-Producing endocrine cells differentiated in vitro from human embryonic stem cells function in macroencapsulation devices in vivo. Stem Cells Transl. Med. *4*, 1214–1222, https://doi.org/10.5966/sctm.2015-0079.

Alagpulinsa, D.A., Cao, J.J.L., Driscoll, R.K., Sîrbulescu, R.F., Penson, M.F.E., Sremac, M., Engquist, E.N., Brauns, T.A., Markmann, J.F., Melton, D.A., and Poznansky, M.C. (2019). Alginate microencapsulation of human stem cell-derived beta cells with CXCL12 prolongs their survival and function in immunocompetent mice without systemic immunosuppression. Am. J. Transpl. *19*, 1930–1940, https://doi.org/10.1111/ajt.15308.

Amer, L.D., and Bryant, S.J. (2016). The *in vitro* and *in vivo* response to MMP-sensitive poly(ethylene glycol) hydrogels. Ann. Biomed. Eng. *44*, 1959–1969, https://doi.org/10.1007/s10439-016-1608-4.

Berman, D.M., Molano, R.D., Fotino, C., Ulissi, U., Gimeno, J., Mendez, A.J., Kenyon, N.M., Kenyon, N.S., Andrews, D.M., Ricordi, C., and Pileggi, A. (2016). Bioengineering the endocrine pancreas: intraomental islet transplantation within a biologic resorbable scaffold. Diabetes *65*, 1350–1361, https://doi.org/10.2337/db15-1525.

Bochenek, M.A., Veiseh, O., Vegas, A.J., McGarrigle, J.J., Qi, M., Marchese, E., Omami, M., Doloff, J.C., Mendoza-Elias, J., Nourmohammadzadeh, M., et al. (2018). Alginate encapsulation as long-term immune protection of allogeneic pancreatic islet cells transplanted into the omental bursa of macaques. Nat. Biomed. Eng. *2*, 810–821, https://doi.org/10.1038/s41551-018-0275-1.

Buchwald, P., Tamayo-Garcia, A., Manzoli, V., Tomei, A.A., and Stabler, C.L. (2018). Glucose-stimulated insulin release: parallel perifusion studies of free and hydrogel encapsulated human pancreatic islets. Biotechnol. Bioeng. *115*, 232–245, https://doi.org/10.1002/bit.26442.

Doloff, J.C., Veiseh, O., Vegas, A.J., Tam, H.H., Farah, H., Ma, M., Li, J., Bader, A., Chiu, A., Sadraei, A., Dasilva, S.A., et al. (2017). Colony stimulating factor-1 receptor is a central component of the foreign body response to biomaterial implants in rodents and non-human primates. Nat. Mat. *16*, 671–680, https://doi.org/10.1038/nmat4866.

Elliott, R.B., Escobar, L., Tan, P.L., Muzina, M., Zwain, S., and Buchanan, C. (2007). Live encapsulated porcine islets from a type 1 diabetic patient 9.5 yr after xenotransplantation. Xenotransplantation *14*, 157–161, https://doi.org/10.1111/j.1399-3089.2007.00384.x.

Ellis, C.E., Vulesevic, B., Suuronen, E., Yeung, T., Seeberger, K., and Korbutt, G.S. (2013). Bioengineering a highly vascularized matrix for the ectopic transplantation of islets. Islets *5*, 216–225, https://doi.org/10.4161/isl.27175.

Farah, S., Doloff, J.C., Müller, P., Sadraei, A., Han, H.J., Olafson, K., Vyas, K., Tam, H.H., Hollister-Lock, J., Kowalski, P.S., et al. (2019). Long-term implant fibrosis prevention in rodents and non-human primates using crystallized drug formulations. Nat. Mater. *18*, 892–904, https://doi.org/10.1038/s41563-019-0377-5.

Fukuda, S., Yabe, S.G., Nishida, J., Takeda, F., Nashiro, K., and Okochi, H. (2019). The intraperitoneal space is more favorable than the subcutaneous one for transplanting alginate fiber containing iPS-derived islet-like cells. Regen. Ther. *11*, 65–72, https://doi.org/10.1016/j.reth.2019.05.003.

Gruessner, A.C., and Sutherland, D.E. (2005). Pancreas transplant outcomes for United States (US) and non-US cases as reported to the united Network for organ sharing (UNOS) and the international pancreas transplant registry (IPTR) as of June 2004. Clin. Transpl. *19*, 433–455, https://doi.org/10.1111/j.1399-0012.2005.00378.x.

Hampson, F.A., Freeman, S.J., Ertner, J., Drage, M., Butler, A., Watson, C.J., and Shaw, A.S. (2010). Pancreatic transplantation: surgical technique, normal radiological appearances and complications. Insights Imaging *1*, 339–347, https://doi.org/10.1007/s13244-010-0046-3.

Hirsch, I.B. (1999). Type 1 diabetes mellitus and the use of flexible insulin regimens. Am. Fam. Physician *60*, 2343–2346. https://www.aafp.org/afp/1999/1115/p2343.html.

Hogrebe, N.J., Augsornworawat, P., Maxwell, K.G., Velazco-Cruz, L., and Millman, J.R. (2020). Targeting the cytoskeleton to direct pancreatic differentiation of human pluripotent stem cells. Nat. Biotechnol. *38*, 460–470, https://doi.org/10.1038/s41587-020-0430-6.

Kikawa, K., Sakano, D., Shiraki, N., Tsuyama, T., Kume, K., Endo, F., and Kume, S. (2014). Beneficial effect of insulin treatment on islet transplantation outcomes in akita mice. PLoS One *9*, e95451, https://doi.org/10.1371/journal.pone.0095451.

Li, R.H., Altreuter, D.H., and Gentile, F.T. (1995). Transport characterization of hydrogel matrices for cell encapsulation. Biotechnol. Bioeng. *50*, 365–373, https://doi.org/10.1002/(SICI)1097-0290(19960520)50:4<365::AID-BIT3>3.0.CO;2-J.

Liu, Q., Chiu, A., Wang, L.H., An, D., Zhong, M., Smink, A.M., de Haan, B.J., de Vos, P., Keane, K., Vegge, A., et al. (2019). Zwitterionically modified alginates mitigate cellular overgrowth for cell encapsulation. Nat. Commun. *10*, 5262, https://doi.org/10.1038/s41467-019-13238-7.

Ma, M., Chiu, A., Sahay, G., Doloff, J.C., Dholakia, N., Thakrar, R., Cohen, J., Vegas, A., Chen, D., Bratlie, K.M., et al. (2013). Core-shell hydrogel microcapsules for improved islets encapsulation. Adv. Healthc. Mater. *2*, 667–672, https://doi.org/10.1002/adhm.201200341.

McBane, J.E., Vulesevic, B., Padavan, D.T., McEwan, K.A., Korbutt, G.S., and Suuronen, E.J. (2013). Evaluation of a collagen-chitosan hydrogel for potential use as a pro-angiogenic site for islet transplantation. PLoS One *8*, e77538, https://doi.org/10.1371/journal.pone.0077538.

Onoe, H., Okitsu, T., Itou, A., Kato-Negishi, M., Gojo, R., Kiriya, D., Sato, K., Miura, S., Iwanaga, S., Kuribayashi-Shigetomi, K., et al. (2013). Metre-long cell-laden microfibres exhibit tissue morphologies and functions. Nat. Mater. *12*, 584–590, https://doi.org/10.1038/nmat3606.

Pagliuca, F.W., Millman, J.R., Gürtler, M., Segel, M., Van Dervort, A., Ryu, J.H., Peterson, Q.P., Greiner, D., and Melton, D.A. (2014). Generation of functional human pancreatic β cells in vitro. Cell *159*, 428–439, https://doi.org/10.1016/j.cell.2014.09.040.

Park, C.G., Bottino, R., and Hawthorne, W.J. (2015). Current status of islet xenotransplantation. Int. J. Surg. *23*, 261–266, https://doi.org/10.1016/j.ijsu.2015.07.703.

Rezania, A., Bruin, J.E., Arora, P., Rubin, A., Batushansky, I., Asadi, A., O'Dwyer, S., Quiskamp, N., Mojibian, M., Albrecht, T., et al. (2014). Reversal of diabetes with insulin-producing cells derived in vitro from human pluripotent stem cells. Nat. Biotechnol. *32*, 1121–1133, https://doi.org/10.1038/nbt.3033.

Sphapiro, A.M., Ricordi, C., Hering, B.J., Auchincloss, H., Lindblad, R., Robertoson, R.P., Secchi, A., Brendel, M.D., Berney, T., Brennan, D.C., et al. (2006). International trial of the Edmonton protocol for islet transplantation. N. Engl. J. Med. *355*, 1318–1330, https://doi.org/10.1056/NEJMoa061267.

Swinnen, S.G., Hoekstra, J.B., and DeVries, J.H. (2009). Insulin therapy for type 2 diabetes. Diabetes Care *32*, 253–259, https://doi.org/10.2337/dc09-S318.

Tomei, A.A., Manzoli, V., Fraker, C.A., Giraldo, J., Velluto, D., Najjar, M., Pileggi, A., Molano, R.D., Ricordi, C., Stabler, C.L., and Hubbell, J.A. (2014). Device design and materials optimization of

conformal coating for islets of Langerhans. Proc. Natl. Acad. Sci. U S A *111*, 10514, https://doi.org/10.1073/pnas.1402216111.

Torren, C., Zaldumbide, A., Duinkerken, G., Schaaf, S., Peakman, M., Stangé, G., Martinson, L., Kroon, E., Brandon, E., Pipeleers, D., and Roep, B. (2017). Immunogenicity of human embryonic stem cell-derived beta cells. Diabetologia *60*, 126–133, https://doi.org/10.1007/s00125-016-4125-y.

Vegas, A.J., Veiseh, O., Gürtler, M., Millman, J.R., Pagliuca, F.W., Bader, A.R., Doloff, J.C., Li, J., Chen, M., Olejnik, K., et al. (2016). Long-term glycemic control using polymer-encapsulated human stem cell-derived beta cells in immune-competent mice. Nat. Med. *22*, 306–311, https://doi.org/10.1038/nm.4030.

Veiseh, O., Doloff, J.C., Ma, M., Vegas, A.J., Tam, H.H., Bader, A.R., Li, J., Langan, E., Wyckoff, J., Loo, W.S., et al. (2015). Size- and shape-dependent foreign body immune response to materials implanted in rodents and non-human primates. Nat. Mater. *14*, 643–651, https://doi.org/10.1038/nmat4290.

Watanabe, T., Okitsu, T., Ozawa, F., Nagata, S., Matsunari, H., Nagashima, H., Nagaya, M., Teramae, H., and Takeuchi, S. (2020). Millimeter-thick xenoislet-laden fibers as retrievable grafts mitigate foreign body reactions for long-term glycemic control in mice. Biomaterials *225*, 120162, https://doi.org/10.1016/j.biomaterials.2020.120162.

Weaver, J.D., Headen, D.M., Hunckler, M.D., Coronel, M.M., Stabler, C.L., and García, A.J. (2018). Design of a vascularized synthetic poly(ethylene glycol) macroencapsulation device for islet transplantation. Biomaterials *172*, 54–65, https://doi.org/10.1016/j.biomaterials.2018.04.047.

Yabe, S.G., Fukuda, S., Nishida, J., Takeda, F., Nashiro, K., and Okochi, H. (2019). Induction of functional islet-like cells from human iPS cells by suspension culture. Regenerative Ther. *10*, 69–76, https://doi.org/10.1016/j.reth.2018.11.003.

Yang, J., Jiang, S., Guan, Y., Deng, J., Lou, S., Feng, D., Kong, D., and Li, C. (2019). Pancreatic islet surface engineering with a starPEG-chondroitin sulfate nanocoating. Biomater. Sci. *7*, 2308, https://doi.org/10.1039/c9bm00061e.

iScience, Volume *24*

Supplemental information

Lotus-root-shaped cell-encapsulated construct as a retrieval graft for long-term transplantation of human iPSC-derived β-cells

Fumisato Ozawa, Shogo Nagata, Haruka Oda, Shigeharu G. Yabe, Hitoshi Okochi, and Shoji Takeuchi

Supplemental Information for

Lotus-root-shaped cell-encapsulated construct as a retrieval graft for long-term transplantation of human iPSC-derived β-cells

Authors: Fumisato Ozawa[1], Shogo Nagata[1], Haruka Oda[2], Shigeharu G. Yabe[3], Hitoshi Okochi[3], and Shoji Takeuchi[1,2,4,*]

[*]Correspondence to: takeuchi@hybrid.t.u-tokyo.ac.jp

This PDF file includes:
Transparent Methods
Figs. S1 to S8

Other Supplementary Materials for this manuscript include the following:

Movies S1, S2, S3 and S4

Transparent Methods

Materials

Barium chloride ($BaCl_2$), sodium chloride (NaCl), potassium chloride (KCl), potassium dihydrogen phosphate (KH_2PO_4), sodium hydroxide (NaOH), calcium chloride ($CaCl_2$), sodium hydrogel carbonate ($NaHCO_3$), bovine serum albumin (BSA), and streptozotocin (STZ) were purchased from Wako Pure Chemical Industries (Japan). D-mannitol, 4-(2-hydroxyethyl)-1-piperazineethanesulfonic acid (HEPES) and fluorescein isothiocyanate-labeled dextran (FITC-labeled dextran) were procured from Sigma-Aldrich Japan (Japan). Hank's balanced salt solution (10×, HBSS) was purchased from Life Technologies. Glucose and magnesium sulfate ($MgSO_4$) were obtained from Nacalai Tesque (Japan). Laminin 511 solution (Imatrix) was obtained from Nippi (Japan). All chemicals were used without further purification. Water was deionized to 18 M ohm cm with a Millipore purification system.

Animals

Immunocompetent male C57BL/6NCrSlc mice for transplantation experiments were obtained from Sankyo Labo Service Corporation, Inc. (Japan). Immunodeficient male NOD-Scid mice were obtained from CLEA Japan, Inc. (Japan). We did not perform randomization in animal studies and randomly assigned mice to each group. All animals were treated in accordance with the policies of the University of Tokyo Institutional Animal Care and Use Committee (Permission number: 29-8).

Fabrication of multi-coaxial microfluidic device

A multi-coaxial microfluidic device consisting of a glass tube, six glass capillaries, and connectors was constructed. Using a puller (PC-10, Narishige, Tokyo, Japan), six

cylindrical glass capillaries (outer diameter: 1.5 mm; inner diameter: 0.9 mm, G-1.5, Narishige, Tokyo, Japan) were pulled to form tapered tips approximately ~600 μm in diametery. These six capillaries were inserted into cylindrical glass tubes (outer diameter: 8.0 mm; inner diameter: 6.0 mm, AS ONE Co. Osaka, Japan) via connectors fabricated using stereolithography (Perfactory, envisionTEC, Marl, Germany).

Optimization of LENCON

To determine the cell position from the edge, 6 mm-thick fibers encapsulating hSC-βs with a randomized cell position in the hydrogel were fabricated using a fluidic device. After fabrication, the fibers were immersed in a culture medium and cultured at 37 °C in a humidified atmosphere of 5% CO_2 and 95% air for 1 week. After the culturing process was complete, we prepared HE sections of the 6 mm-thick fibers as described below and then evaluated their viability by calculating the ratio of enucleated cells and cells in the HE sections. The cell area obtained by subtracting the enucleated cell area from the area of all stained cells was used as the live cell area. Image analysis was performed using ImageJ, RGB split processing was performed on the HE section images, and the blue and red spheroid areas were defined as the enucleated cell area and the area of all stained cells, respectively.

Differentiation of hSC-β

The human iPSC line, TkDN4-M, provided by Dr. M. Ohtsu at The Institute of Medical Science, The University of Tokyo, was used. Freeze-stored iPSCs were thawed and cultured in a hiPS medium (DMEM/Ham's F12; Wako) in the presence of 20% knockout serum replacement (KSR; GIBCO), 1× non-essential amino acids (NEAA; Wako), 55 mM 2-mercaptethanol (2-ME, GIBCO), and 7.5 ng/ml recombinant human fibroblast growth factor 2 (FGF2) (Peprotech) on mitomycin-C (Wako)-treated SNL feeder cells to maintain an undifferentiated state. Cultured iPSCs were dissociated with CTK solution and seeded at a density of 1×10^6 cells/ml in a spinner type reactor (Biott) containing 30 ml of mTeSR 1 (Veritas) with 10 mM ROCK inhibitor (Y-27632; Cayman Chemical) at a rotation rate of 45 rpm. Spheroids formed due to cell aggregation during the 2-day culture were then cultured in hiPS medium for 1 day before starting differentiation. The differentiation protocols comprised six stages and were performed (S. G. Yabe et al. 2019).

At stage 1 (DE: definitive endoderm), spheroids were cultured for 4 days in RPMI 1640 (Wako) supplemented with 0.25% bovine serum albumin (BSA; Sigma), 0.4× penicillin and streptomycin (PS; Wako), 1 mM sodium pyruvate (Wako), 1× NEAA, 80 ng/ml recombinant human activin A (Peprotech) and 55 μM 2-ME. Fifty ng/ml FGF2, and 20 ng/ml recombinant bone morphogenetic protein 4 (BMP4; Peprotech) and 3 μM CHIR-99021 (Biovision) were added for the first 2 days, and 0.5% KSR was added on day 4.

At stage 2 (PGT: primitive gut tube), spheroids were cultured for 3 days in RPMI 1640 supplemented with 0.25% BSA, 1 mM sodium pyruvate, 1× NEAA, 0.4× PS, and 50 ng/ml recombinant human FGF7 (Peprotech), 1% B27 supplement (GIBCO) and 1:333 insulin, transferrin, selenium, ethanolamine solution (ITS-X; Gibco). The medium was changed on the third day.

At stage 3 (PFG: posterior fore gut), spheroids were cultured in DMEM (8 mM glucose) supplemented with 0.15% BSA, 0.4× PS, 1× NEAA, 50 ng/ml FGF7,1% B27 supplement,

1:333 ITS-X, 0.5 µM EC23 (Santa Cruz Biotechnology), 0.2 µM LDN 193189 (Cayman Chemical), 0.3 µM indolactam V (ILV; Cayman Chemical), and 0.25 µM SANT1 (Cayman Chemical) for 4 days. The medium was changed every 2 days during stage 3.

At stage 4 (PP: pancreatic progenitor), spheroids were cultured in DMEM (8 mM glucose) supplemented with 0.15% BSA, 0.4× PS, 1× NEAA, 50 ng/ml recombinant human FGF10 (Peprotech), 1% B27 supplement, 1:333 ITS-X, 0.04 µM EC23, 0.2 µM LDN 193189, 0.3 µM ILV, and 0.25 µMSANT1, 10 mMAlk5 inhibitor II (Rep Sox; Biovision) and 5 µM ZnSO4 (Sigma) for 3 days. The medium was changed on the third day.

At stage 5 (EP: endocrine progenitor), spheroids were cultured in DMEM (20 mM glucose) supplemented with 0.15% BSA, 0.4× PS, 1× NEAA, 20 ng/ml recombinant human epidermal growth factor (EGF; Peprotech), 1% B27 supplement, 1:333 ITS-X, 0.02 µM EC23, 0.2 µM LDN 193189, 0.25 µM SANT1, 10 µM Rep Sox, 5 µM ZnSO4, 50 ng/ml exendin-4 (Abcam), 10 µg/ml heparin (Sigma), 10 µM Y27632, 0.5 µM DBZ (Cayman Chemical) and 5 µM Nicotinamide (Sigma) for 7 days; the medium was changed every 2 days during stage 5.

At stage 6 (BETA: bcell stage), spheroids were cultured in DMEM (20 mM glucose) supplemented with 0.15% BSA, 0.4× PS, 1× NEAA, 1% B27 supplement, 1:333 ITS-X,10 µM Rep Sox, 5 µM ZnSO4, 50 ng/ml exendin-4, 10 µg/ml heparin, 5 µM Nicotinamide, 10 ng/ml BMP4, 50 ng/ml recombinant human hepatocyte growth factor (HGF; Peprotech), 50 ng/ml insulin-like growth factor 1 (IGF-1; Peprotech) and 5 µM forskolin (Wako) for 10 days. The mediumwas changed every 2 days during stage 6. We added 1 µM R428 (Cayman Chemical) to the medium of batch C.

Fabrication of LENCON encapsulating hSC-β

LENCONs were prepared using the microfluidic device. The hSC-β suspension dispersed in 0.5% sodium alginate (ALG100, Mochida Pharmaceutical Co. Ltd., Tokyo, Japan) and dissolved in 0.9% saline containing 333 ng/ml laminin was used as a core solution. The shell solution employed was 1.3% sodium alginate (ALG500, Mochida Pharmaceutical Co. Ltd., Tokyo, Japan) dissolved in 0.9% saline containing 0.25% sodium hyaluronate. The role of laminin is the scaffold protein of hSC-βs, and the role of the sodium hyaluronate is the anti-inflammatory effect *in vivo*. These solutions were sterilized in a syringe filter unit with a pore size of 0.22 µm (MILLEX-GP, MerckMillipore, Japan). The gelling solution was $BaCl_2$ (20 mM $BaCl_2$, 250 mM D-Mannitol, 25 mM HEPES), which was sterilized using an autoclave. Prior to loading these solutions into the microfluidic device, the device and tubes were sterilized by washing them with 70% ethanol for 10 min. The solutions were infused into the device at constant flow rates to generate a multi coaxial laminar flow in the device (Fig. S1). The typical flow rates of the core and shell streams were as follows: Q_{core} = 50 µL/min and Q_{shell} = 1200 µL/min, respectively. The LENCON extruded into a chamber filled with 100 mM $CaCl_2$ solution as follows 3 steps. At first step, the shell solution was introduced into the device for sealing. At second step, the core solution was introduced while flowing the shell solution. Third step, the core solution was stopped and the shell solution continuously introduced for sealing again. After the hydrogel was formed, it was gelled in a $BaCl_2$ gelling solution (20 mM $BaCl_2$, 250 mM D-Mannitol, and 25 mM HEPES) for 1 h at 4 ℃ and then transferred into 0.9% saline solution for removing the remaining non-gelling $BaCl_2$. The LENCONs were then

immersed in the culture medium and cultured at 37 °C in a humidified atmosphere of 5% CO_2 and 95% air for 1 day to set.

Fabrication of 1 mm-thick graft encapsulating hSC-β

To produce 1 mm-thick grafts encapsulating hSC-βs, the microfluidic device was fabricated by using glass capillaries and connectors (T. Watanabe et al. 2020). The device and all tubing sections were sterilized by washing them with 70% ethanol for 10 min. The solutions were infused into the device at constant flow rates to generate a double coaxial laminar flow in the device. The typical flow rates of each stream core, shell, and gelling were as follows: Q_{core} = 50 μL/min, Q_{shell} = 350 μL/min, and $Q_{gelling}$ = 3600 μL/min, respectively. The 1 mm-thick fibers generated in the device were collected in a tube filled with a $BaCl_2$ gelling solution. After the grafts were formed, they were incubated in a collection bath for 10 min and then transferred to a culture dish filled with 0.9% saline to remove the remaining non-gelling $BaCl_2$. The grafts were then immersed in the culture medium and cultured at 37 °C in a humidified atmosphere of 5% CO_2 and 95% air for 1 day to set.

Evaluation of the effect of graft diameter on cellular deposition *in vivo*

The 1 mm-thick grafts and LENCONs were transferred to a culture dish filled with 0.9% saline to remove the medium components and were then implanted into the intraperitoneal space of a non-diabetic eight-week-old male C57BL/6NCvSlc mice weighing 20–26 g. The grafts were implanted every 2 months, 4 months, and 1 year, following which, each graft was retrieved from the intraperitoneal space using tweezers. During implantation and retrieval, the mice were anaesthetized using isoflurane (Forane, Abbott) at a concentration of 4–5% for induction and 2% for maintenance using Univentor 400 (Univentor, MALTA). The retrieved grafts were washed with 0.9% saline. After washing, each graft was analyzed using histological analysis and rheology.

Rheological measurement of grafts

The rheological measurements were conducted using an Anton-Paar MCR 302 Rheometer (Anton Paar, Graz, Austria). The parallel plate (D-CP/PP7) was substituted with a 3D printed disposable plate to match the diameters of the samples (1 mm and 6 mm). Note that the sample of 1 mm fiber after 1 year transplantation could not be measured due to the graft retrieval from the intraperitoneal space (NA). The temperature of the measuring system was maintained at 25 °C by using a water bath combined with a Peltier heating system. All the samples were delivered in a saline solution within 2 h of retrieval. The samples were then sliced with a blade to a thickness of approximately 1.5 mm. The samples were then placed under the parallel plate, which was lowered until it attained a gap distance of 1.0 mm. The storage and loss moduli of the sample were measured while varying the frequency from 100 rad/s to 0,1 rad/s exponentially for 22 points. The storage modulus (G′), loss modulus (G″), loss tangent (tan δ = G″/G′), and complex viscosity as functions of frequency were continuously determined during the measurement. All the measurements were obtained thrice and were conducted within 4 h of sample arrival. For every sample, a storage and loss modulus of 2.68 rad/s was selected as a representative value for comparison.

Histological analysis of grafts

The grafts were added to saline containing 4% paraformaldehyde overnight at 4 °C , and then the fixed grafts were dehydrated, embedded in OCT compound, and cryosectioned using conventional procedures. The cryosectioned grafts were subjected to HE staining and immunostaining. For HE staining, the cryosectioned grafts were stained with Mayer's hematoxylin and 0.5% eosin Y ethanol solution.

For immunostaining, the cryosectioned grafts were washed with saline solution and pre-treated with blocking buffer [5% BSA in PBST (PBS with 0.1% Triton X-100)] overnight at 4 °C. The grafts were immunoreacted with anti-C-peptide (pancreatic cell function marker, abcam, ab14181), anti-Glucagon (pancreatic α cell function marker, abcam, ab10988), anti-NKX6.1 (the earliest marker of pancreatic β cell, abcam, ab221549), anti-Insulin (pancreatic β cell function marker, Novus Biologicals, NBP2-15195), anti-F4/80 antibody (macrophage marker, Bio-Rad Laboratories, MCA497GA), and anti-αSMA antibody (a marker for a subset of activated fibrogenic cells and myofibroblasts, abcam, ab5694) in the antibody buffer [1% BSA in PBST] overnight at 4 °C and incubated with secondary antibodies in the antibody buffer for 1 h.

Glucose-stimulated insulin secretion

In vitro glucose responsive insulin secretion of hSC-βs was measured using the glucose-stimulated insulin secretion assay, which was conducted before transplantation and after retrieval. The LENCON were preincubated for 1 h at 37 °C in HKRB solution (HEPES-added Krebs-Ringer bicarbonate buffer; 134 mM NaCl, 4.7 mM KCl, 1.2 mM KH_2PO_4, 2 mM $CaCl_2$, 1.2 mM $MgSO_4$, 0.5% BSA, and 10 mM HEPES with NaOH (pH 7.4)) containing 3.3 mM glucose. The grafts were incubated for 1 h each at 37 °C in HKRB solutions containing 3.3, 22.2, and 3.3 mM glucose for the low, high, and second low glucose stimulations, respectively. The total amount of insulin released into each HKRB solution during the incubation was determined using Mercodia Ultrasensitive human C-peptide ELISA (Mercodia, Sweden) and Mercodia Ultrasensitive human glucagon ELISA (Mercodia, Sweden), according to the manufacturer's protocols.

***In vivo* function and morphology of LENCON into immunodeficient mice**

To ensure fewer transplant rejections, we first selected NOD-Scid mice, which are commonly used (P. Mezquita et al. 2008) as the xenotransplantation model, to assay human candidate cells. The LENCON encapsulated 6×10^6 cells of hSC-βs into the core region. Eight-week-old male NOD-Scid mice weighing 20–26 g were rendered diabetic using a single intraperitoneal injection of 120 mg/kg STZ. Following the STZ injection, if the blood glucose concentration exceeded 350 mg/dL (hyperglycemia) for two consecutive days, the mice were diagnosed to be diabetic. The mice were anaesthetized with 4–5% isoflurane (Forane, Abbott) concentration for induction and 2% for maintenance using Univentor 400 (Univentor, MALTA). Preoperatively, all mice received 0.9% saline subcutaneously to prevent dehydration. The abdomens of the mice were shaved and ~1 cm incision was created for each using scissors. The grafts were then transplanted into the intraperitoneal space of normal or STZ-induced diabetic C57BL/6NCvSlc mice. After transplantation, the skin was closed over the incision using a wound clip. The blood glucose concentrations of STZ-induced diabetic mice transplanting grafts were measured using a glucose monitoring system (ACCU-CHEK Active; Roche Diagnostics) at least every three days throughout the experiment. Mice with non-fasting blood glucose concentrations below 200 mg/dL were considered normoglycemic.

Following the transplantation, the recipient blood was collected every 2, 12, and 28 weeks; further, C-peptide concentrations in the blood were measured using ELISA. To evaluate the efficacy of the grafts after transplantation, an oral glucose tolerance test (OGTT) was conducted 7 day before retrieval. For comparison, the OGTT was also conducted on the diabetic and non-diabetic control mouse groups. After 10 h of fasting, a glucose solution (2 g glucose/kg body weight) was added into the intraperitoneal space of the mice. The blood glucose concentrations of the recipients were monitored 0, 15, 30, 60, 90, and 120 min after glucose addition. To perform a second-look laparotomy, the mice were anesthetized. An incision was made in the skin of the abdomen, and the intraperitoneal wall and space containing the grafts were exposed. The morphology of the grafts was observed by using a microscope. The grafts were then retrieved from the intraperitoneal space using tweezers (day 54, 120, 127, 131, 180); we gripped the grafts with the tweezers, picked them up, and transferred them from inside to outside the intraperitoneal cavity. The retrieved grafts were fixed in 4% paraformaldehyde overnight. The fixed samples were then dehydrated and embedded in OCT compound using conventional procedures. Frozen sections (8 μm thick) were stained using HE and immunofluorescence analysis was performed. The prepared sections were observed with an upright microscope (BX51WI, Olympus, Japan).

Long-term transplantation of LENCON into immunocompetent mice

The LENCON encapsulated 6×10^6 cells of hSC-βs into the core region. Eight-week-old male C57BL/6NCvSlc mice weighing 20–26 g were rendered diabetic using a single intraperitoneal injection of 120 mg/kg STZ. Following the STZ injection, if the blood glucose concentration exceeded 350 mg/dL (hyperglycemia) for two consecutive days, the mice were diagnosed to be diabetic. The mice were anaesthetized with 4–5% isoflurane (Forane, Abbott) concentration for induction and 2% for maintenance using Univentor 400 (Univentor, MALTA). Preoperatively, all mice received 0.9% saline subcutaneously to prevent dehydration. The abdomens of the mice were shaved and ~1 cm incision was created for each using scissors. The grafts were then transplanted into the intraperitoneal space of normal or STZ-induced diabetic C57BL/6NCvSlc mice. After transplantation, the skin was closed over the incision using a wound clip. The blood glucose concentrations of STZ-induced diabetic mice transplanting grafts were measured using a glucose monitoring system (ACCU-CHEK Active; Roche Diagnostics) at least every three days throughout the experiment. Mice with non-fasting blood glucose concentrations below 200 mg/dL were considered normoglycemic. Following the transplantation, the recipient blood was collected every two weeks and the C-peptide concentrations were measured using ELISA. To perform a second-look laparotomy, mice were anesthetized one year after transplantation for LENCON. An incision was made in the skin of the abdomen, and the intraperitoneal wall and space containing the grafts were exposed. The morphology of the grafts was observed by using a microscope. The grafts were then retrieved from the intraperitoneal space using tweezers; we gripped the grafts with the tweezers, picked them up, and transferred them from inside to outside the intraperitoneal cavity. The retrieved grafts were fixed in 4% paraformaldehyde overnight. The fixed samples were then dehydrated and embedded in OCT compound using conventional procedures. Frozen sections (8 μm thick) were stained using HE and immunofluorescence analysis was performed. The prepared sections were observed with an upright microscope (BX51WI, Olympus, Japan).

Statistical Analysis

Data are expressed as mean ± s.d. Experiments about survival of hSC-βs in 6 mm-thick hydrogel and evaluation of fibrosis formation and mechanical strength of grafts were repeated at least three times. Animal cohorts were randomly selected. Investigating surgeons were blinded to the procedures performed during the transplantation and while retrieving the grafts encapsulating hSC-βs. In addition, data are expressed as mean ± s.d. Experiments about evaluation of long-term transplant function into NOD-Scid mice and C57BL/6 mice were repeated at 3-5 times. GSIS assay data were analyzed for statistical significance using unpaired Student t-test using Excel 365. Data regarding the difference in oral glucose tolerance test (OGTT) were analyzed for statistical significance by Tukey-Kramer multiple comparison test, as implemented in Excel 365; *, **P < 0.01.

References

S. G. Yabe *et al.* (2019), Induction of functional islet-like cells from human iPS cells by suspension culture. *Regenerative Therapy*, **10**, 69-76, https://doi.org/10.1016/j.reth.2018.11.003

T. Watanabe *et al.* (2020), Millimeter-thick xenoislet-laden fibers as retrievable grafts mitigate foreign body reactions for long-term glycemic control in mice. *Biomaterials*, **225**, 120162, https://doi.org/10.1016/j.biomaterials.2020.120162

P Mezquita *et al*. (2008), NOD/SCID repopulating cells contribute only to short-term repopulation in the baboon. *Gene Therapy*, **15**, 1460-1462, https://doi.org/10.1038/gt.2008.108

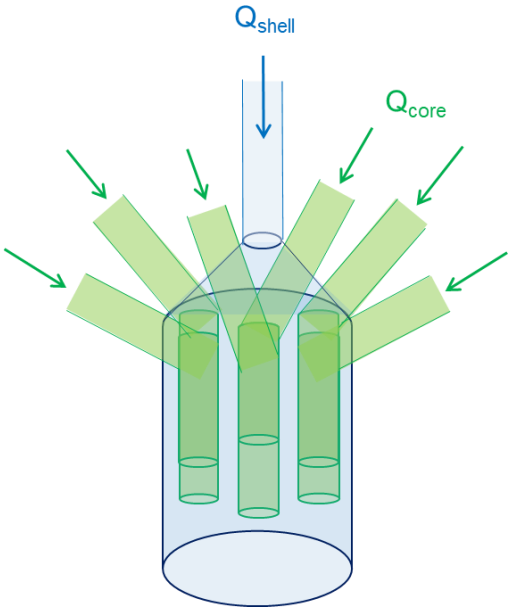

Fig. S1. Schematic of the fluidic device for fabrication of LENCON, Related to Figure 2.

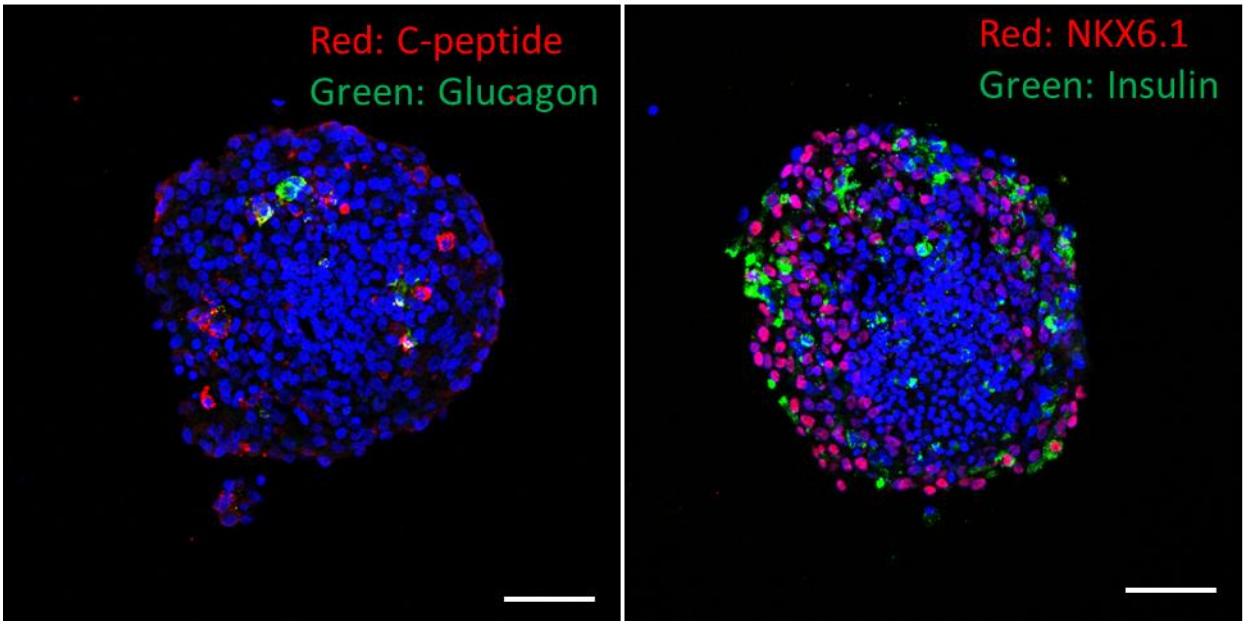

Fig. S2. Immunefluorescent staining image of encapsulating hSC-β, Related to Figure 2. (Scale bar: 100 μm)

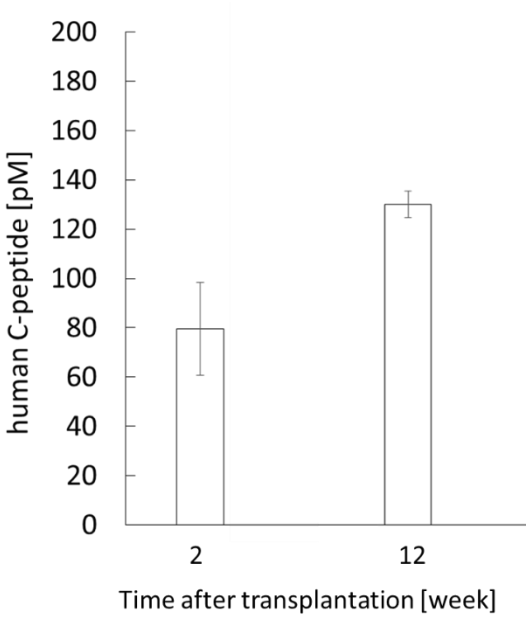

Fig. S3. ELISA results of blood samples of the recipient mice transplanted with 1mm graft, Related to Figure 4.

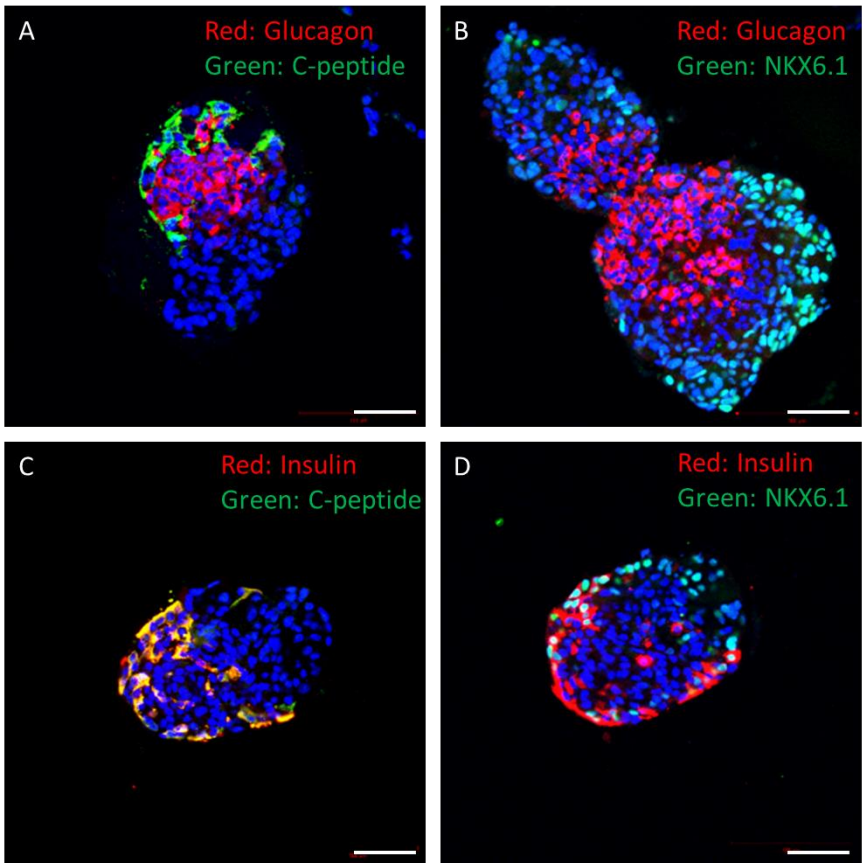

Fig. S4. Retrieved LENCON graft from NOD-SCid mice, Related to Figure 4. Fluorescent images of encapsulated hSC-βs in the stained retrieved grafts with glucagon and insulin in red and C-peptide and NKX6.1 in green. (Scale bar: 50 µm)

Fig. S5. Retrieval of 1 mm-thick fiber after 4-month transplantation, Related to Figure 4. The fiber was broken into pieces. (Scale bar: 1 cm)

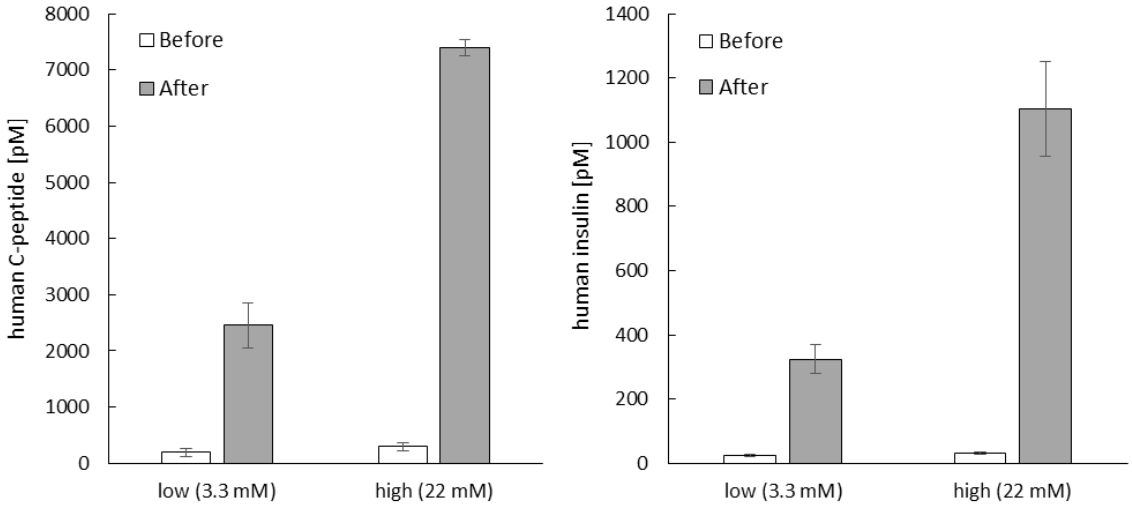

312

313 **Fig. S6. Glucose responsive test of the grafts before and after transplantation into immunodeficient**
314 **NOD-Scid mice, Related to Figure 4.**

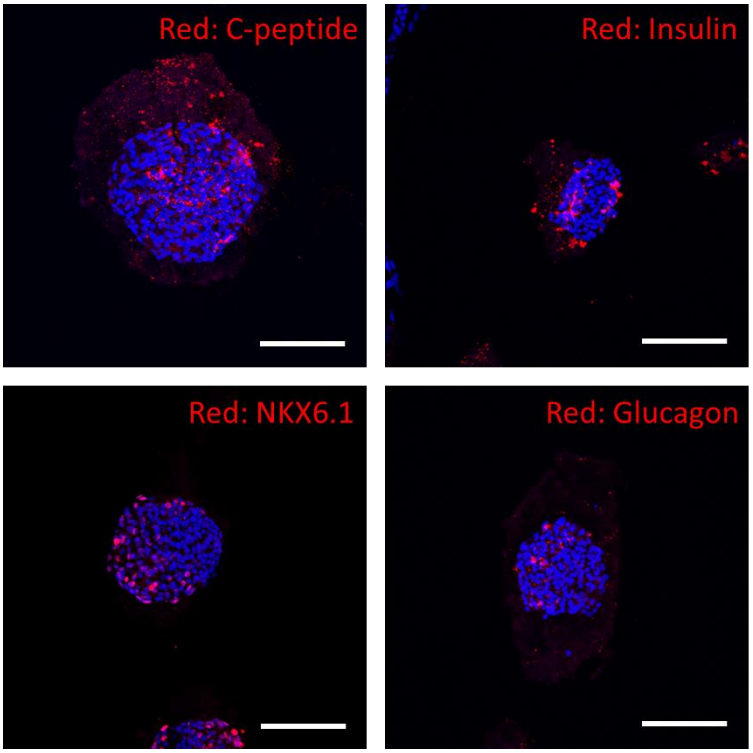

Fig. S7. Retrieved LENCON from C57BL/6 mice, Related to Figure 5. Fluorescent images of encapsulated hSC-βs in the stained retrieved grafts with (A) C-peptide, (B) insulin, (C) NKX6.1, and (D) glucagon. (Scale bar: 50 μm)

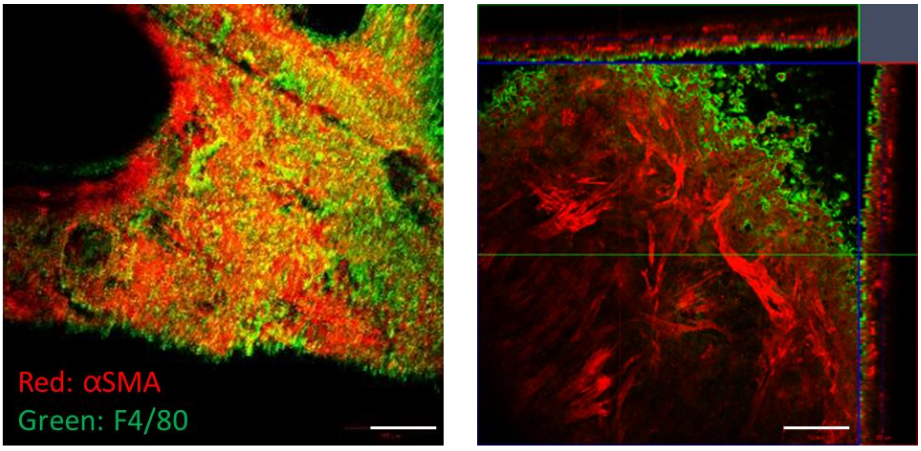

Fig. S8. Immunofluorescent staining of retrieval graft surface, Related to Figure 5. Fluorescent images of the stained retrieved grafts with αSMA in red and F4/80 in green. (Scale bar: 50 μm)